SPECTATOR FRAGMENTATION INDUCED BY RELATIVISTIC ^{12}C PROJECTILES

K.Turzó[6,5] and
G. Auger[1], Ch.O. Bacri[2], M.L. Begemann-Blaich[6], N. Bellaize[3], R. Bittiger[6], F. Bocage[3], B. Borderie[2], R. Bougault[3], B. Bouriquet[1], Ph. Buchet[4], J.L. Charvet[4], A. Chbihi[1], R. Dayras[4], D. Doré[4], D. Durand[3], J.D. Frankland[1], E. Galichet[2], D. Gourio[6], D. Guinet[5], S. Hudan[1], B. Hurst[3], G. Immé[8], Ph. Lautesse[5], F. Lavaud[2], J.L. Laville[1], Ch. Leduc[5], A. Le Fèvre[6], R. Legrain[4], O. Lopez[3], J. Łukasik[6,10], U. Lynen[6], W.F.J. Müller[6], L. Nalpas[4], H. Orth[6], E. Plagnol[2], G. Raciti[8], E. Rosato[9], A. Saija[8], C. Schwarz[6], W. Seidel[7], C. Sfienti[6], J.C. Steckmeyer[3], G. Tabacaru[3], B. Tamain[3], W. Trautmann[6], A. Trczinski[11], E. Vient[3], M. Vigilante[9], C. Volant[4], B. Zwieglinski[11],
(ALADIN and INDRA collaborations)

[1] GANIL, CEA et IN2P3-CNRS, B.P. 5027, F-14076 Caen Cedex, France
[2] Institut de Physique Nucléaire, IN2P3-CNRS, F-91406 Orsay Cedex, France
[3] LPC, IN2P3-CNRS, ISMRA et Université, F-14050 Caen Cedex, France
[4] DAPNIA/SPhN, CEA/Saclay, F-91191 Gif sur Yvette Cedex, France
[5] Institut de Physique Nucléaire, IN2P3-CNRS et Université, F-69622 Villeurbanne Cedex, France
[6] Gesellschaft für Schwerionenforschung, D-64291 Darmstadt, Germany
[7] Forschungszentrum Rossendorf, D-01314 Dresden, Germany
[8] Dipartimento di Fisica dell' Universitá and INFN, I-95129 Catania, Italy
[9] Dipartimento di Scienze fisiche e Sezione INFN, Universita di Napoli "Federico II", I-80126 Napoli, Italy
[10] H. Niewodniczański Institute of Nuclear Physics, Pl-31342 Kraków, Poland
[11] Soltan Institute for Nuclear Studies, Pl-00681 Warsaw, Poland

Abstract

The multifragmentation of highly excited spectator systems was studied with the 4π multidetector INDRA in experiments at the GSI. Data were taken for the reactions ^{12}C+^{197}Au and ^{12}C+^{112,124}Sn at bombarding energies ranging from 95 to 1800 AMeV. High resolution at backward angles, dominated by emissions from the target spectator, was achieved with the Si-Si-CsI(Tl) calibration telescopes of INDRA. First results for ^{12}C+^{197}Au, obtained from inclusive light-particle and fragment spectra, are reported.

1 Introduction

In 1998 and 1999, a series of experiments was conducted at the GSI with the INDRA multidetector [1], using high-energy beams from the heavy-ion synchrotron SIS [2, 3]. A part of these experiments has been dedicated to asymmetric systems like ^{12}C+^{197}Au and ^{12}C+^{112,124}Sn at bombarding energies ranging from 95 to 1800 AMeV. The physics goals in this study of spectator fragmentation are the principal

question of thermal and/or dynamical breakup of the source, and, with the isotopically pure tin targets, the role of the isospin degree of freedom in the fragmentation process.

The study has been partly motivated by previous results obtained by the Aladin collaboration for ^{197}Au+^{197}Au collisions at 600, 800 and 1000 AMeV [4, 5]. The invariance with the bombarding energy that was observed in the fragment channels was one of the prominent features of these data and was interpreted as indicating equilibrium at the breakup stage. On the other hand, the neutron emission at spectator rapidities was found to strongly depend on the bombarding energy which pointed to its origin in the primary dynamical stages of the collision. Two distinctly different behaviours were observed and associated with the excitation and decay stages of the produced spectator system.

In the present study, excitation functions were measured over a wide range of bombarding energies with the idea to use the observed variations for a more systematic distinction of equilibrated from non-equilibrated emissions. The light charged products from the target spectator are particularly important since they carry away a major part of the excitation energy. The quantitative identification of the system at breakup, including the energy content, is essential for the investigation of the fragment formation process and a prerequisite for the application of statistical fragmentation models.

2 Experimental method

The multidetector INDRA consists of 336 telescopes arranged in 17 rings in a 4π geometry with increasing granularity towards smaller angles in the forward hemisphere. The major part of the solid angle ($\theta_{lab} > 45^\circ$) is covered with two-element telescopes consisting of ionisation chambers and CsI(Tl) crystals. In the forward section ($\theta_{lab} < 45^\circ$), silicon detectors of 300 μm thickness are inserted between the ionisation chambers and the CsI(Tl) crystals [1].

The velocity of the target spectators is small at relativistic energies, and their emission nearly isotropic in the laboratory frame while light particles from the initial reaction stages are forward peaked. Consequently, the study of spectator fragmentation is best done at backward angles where, however, a good isotopic resolution with low threshold is only provided by the Si-Si-CsI(Tl) calibration telescopes of INDRA (Fig. 1). These eight telescopes are distributed in the angular range from 45° to 180°, one module per ring, and consist of two circular silicon detectors, a 80-μm detector followed by a Si(Li) detector with thickness 2000 μm, mounted between the ionization chamber and the CsI(Tl) crystal of a telescope module.

The calibration of the first Si detector (80 μm) of these telescopes was obtained with α particles from a ^{212}Pb radioactive source. The calibrations of the following Si and CsI(Tl) detectors were derived from the measured $\Delta E - E$ maps by adjusting to the predictions of energy-loss and range tables.

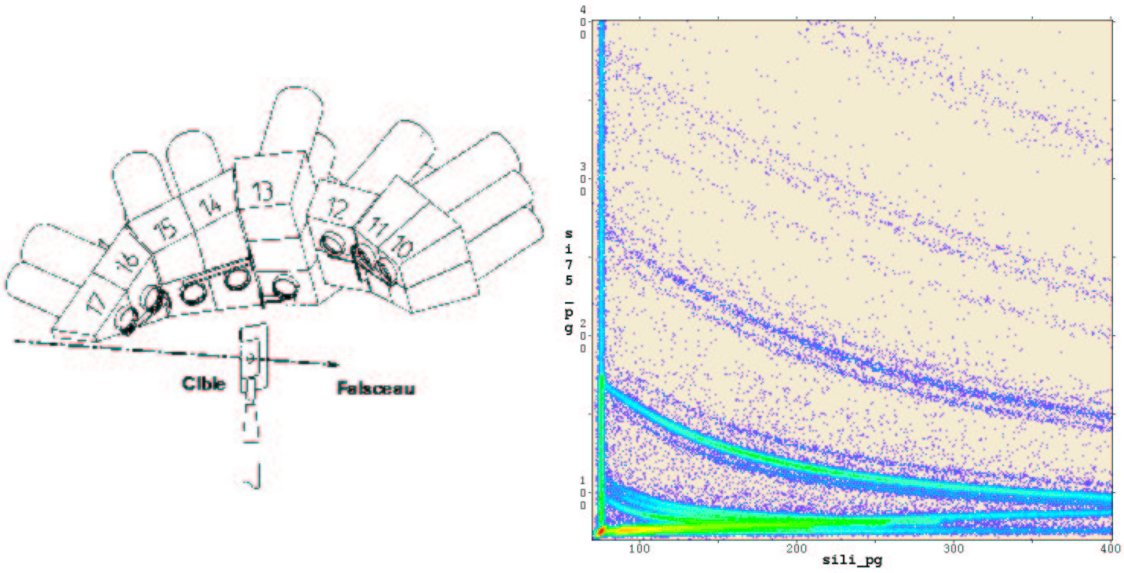

Figure 1: Left-hand side: Mechanical assembly of the 8 Si-Si-CsI(Tl) telescopes in rings 10 to 17 of the INDRA detector ($\theta_{lab} > 45°$). The silicon detectors are represented by the disks in front of the CsI crystals which are facing the target (cible). The dashed line corresponds to the beam (faisceau) axis. Right panel: ΔE-E matrix (in channels) obtained with the Si-Si telescope of ring 11 ($\langle\theta_{lab}\rangle = 65°$), illustrating the achieved isotopic resolution for fragments up to boron.

3 Rapidity distributions

Inclusive rapidity distributions for hydrogen and helium isotopes and for lithium, beryllium and boron ions from the reaction ^{12}C+^{197}Au at 1000 AMeV are shown in Fig. 2. They are integrated over the whole detector with no corrections for its acceptance. Some of the observed structures are therefore of experimental origin. The holes at zero rapidity reflect the gap of $88° \leq \theta_{lab} \leq 92°$ in the INDRA acceptance. The change of the identification threshold at $\theta_{lab} = 45°$ is smeared out on the rapidity scale but may cause some forward-backward asymmetry. The maximum energy of protons stopped in the CsI(Tl) detectors at forward angles is about 240 MeV [1] which limits the proton rapidity distribution to $y \leq 0.7$. At this bombarding energy, the proton energy distributions extend far beyond the detection limit at practically all angles. Therefore, their rapidity distribution, and to some extent also that of other light charged particles, is strongly modified by the acceptance.

Except for the gap at zero rapidity, the distributions of intermediate-mass fragments are less affected by the acceptance limits. They are centered close to zero rapidity and are nearly symmetric. The mean rapidity is about 0.03 for the light lithium, beryllium and boron fragments but decreases to values between 0.01 and 0.02 over the range of intermediate-mass fragments $Z \leq 20$. The assumption of the existence of a common equilibrated source of fragment emission requires identical mean rapidities for all particles emitted from it. However, these are still inclusive results, and it will have to be seen how the rapidity evolves with impact parameter.

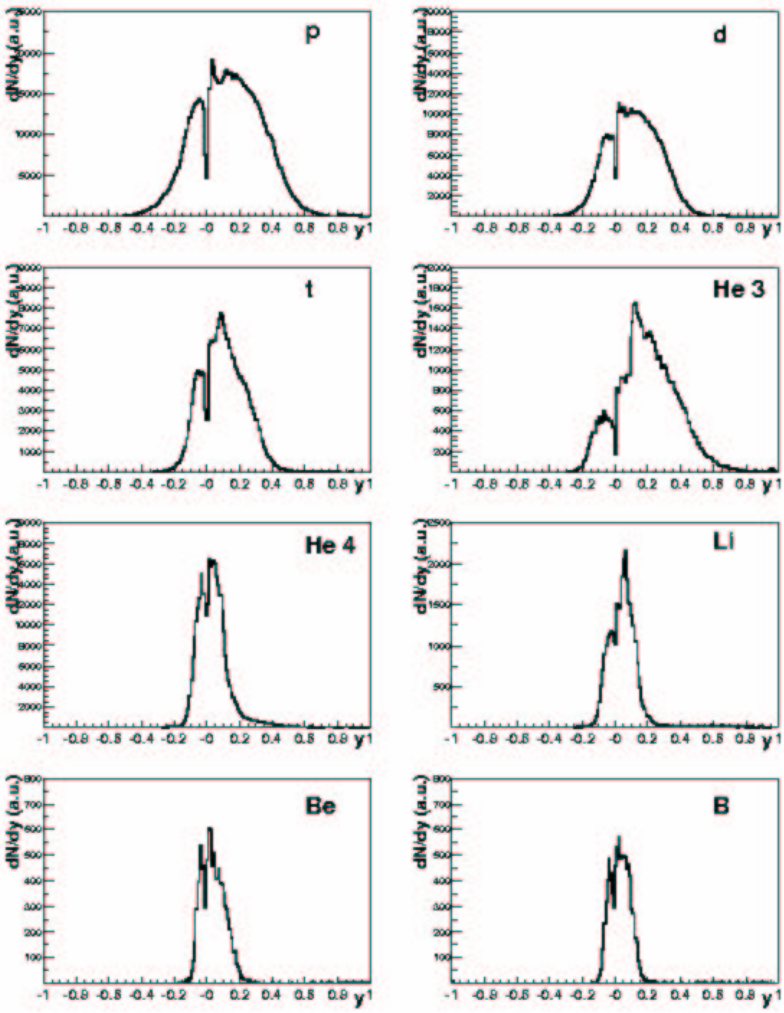

Figure 2: Rapidity distributions in the laboratory frame for protons (p), deuterons (d), tritons (t), ^{3}He, ^{4}He, and lithium, beryllium and boron fragments for ^{12}C+^{197}Au at 1000 AMeV.

Rapidity spectra for the same reaction have been measured in reverse kinematics by the EOS collaboration [6]. For protons and other light particles, the tail towards midrapidity due to the initial cascading stage of the reaction is more clearly visible. The question of the separation of the two stages within a continuous reaction process has been adressed in different ways by other groups [6, 7, 8] who have studied multifragmentation induced by light relativistic projectiles. In the present case, useful criteria are expected to be obtained from the measured dependence on the incident energy.

4 Energy spectra and Temperatures

Energy spectra measured with the calibration telescope of ring 13 ($\langle\theta_{lab}\rangle = 101°$) for protons and ^{7}Li for the full range of bombarding energies 95 to 1800 AMeV are given

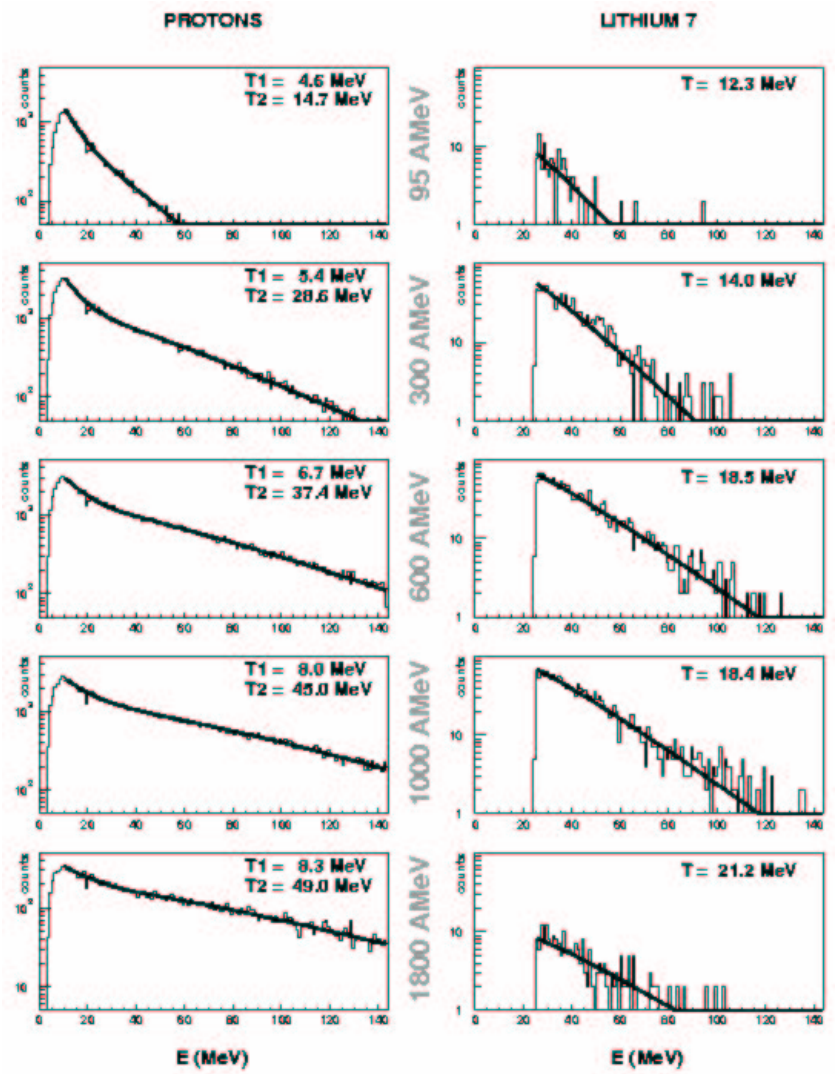

Figure 3: Energy spectra of protons and ^{7}Li fragments measured with the calibration telescope of ring 13 ($\langle\theta_{lab}\rangle = 101°$) for the ^{12}C+^{197}Au reaction from 95 to 1800 AMeV. The full lines represent the results of one-source (^{7}Li) and two-source (p) fits with Maxwell-Boltzmann functions. The obtained slope temperatures are indicated where $T1$ and $T2$, in the proton case, denote the values for the low-temperature and high temperature components, respectively.

in Fig. 3. The thresholds for isotopic identification of 3 MeV and 22 MeV correspond to the energies needed for these particles to penetrate the ionization chamber and the 80-μm detector. The spectra were fitted, as a first approach, with two-parameter Maxwell-Boltzmann functions. A superposition of two such sources was required for the proton spectra which exhibit a low-energy component, probably containing the contributions of evaporation, breakup, and sequential emission, superimposed on the hard component that extends to rather high energies.

The temperatures given by the slopes of these maxwellians show different behaviors. For the low-temperature component of protons ($T1$) and for the ^{7}Li ions, they

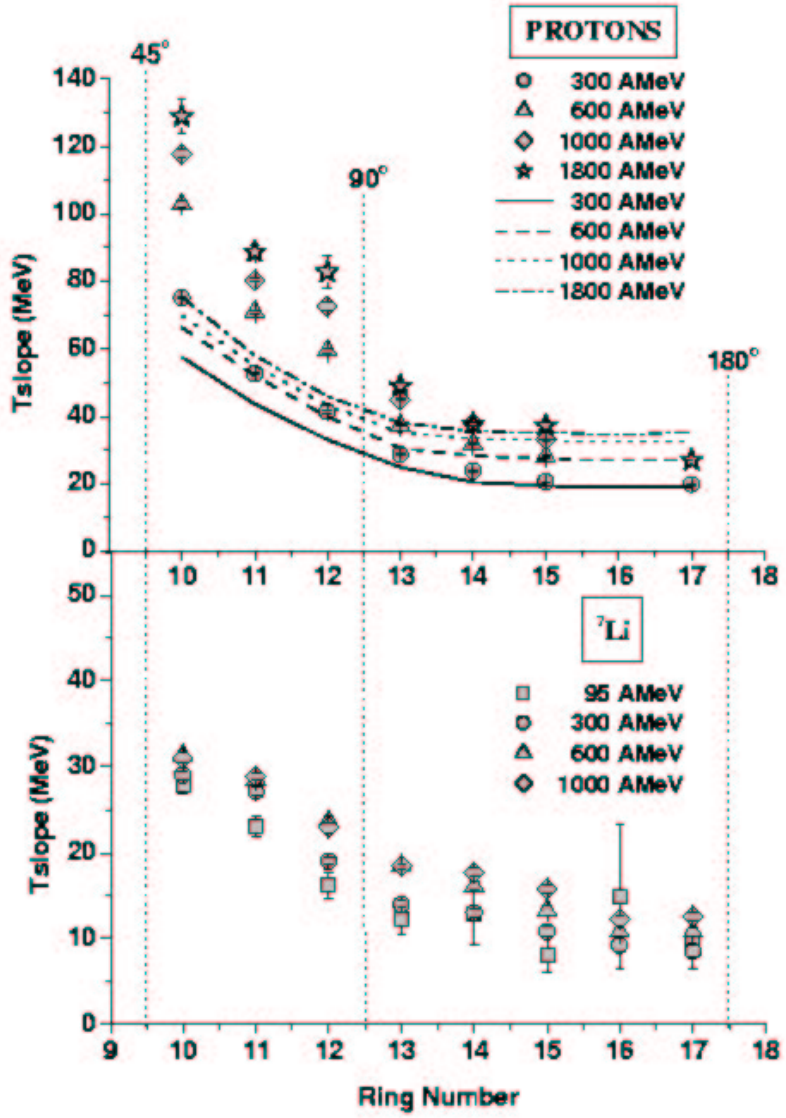

Figure 4: Slope temperatures $T_{\rm slope}$ of protons (top) and ^{7}Li (bottom) as a function of the ring number for ^{12}C+^{197}Au at the indicated bombarding energies. In the proton case, the high-temperature values $T2$ are given and compared with the results of the Gudima-Toneev cascade model (lines).

increase very slowly with the incident energy. The lithium temperatures even seem to reach some saturation near 600 AMeV incident energy, consistent with the invariance of the fragment kinetic energies observed for $3 \leq Z \leq 20$ in the ^{12}C+^{197}Au reaction for 600 to 1000 AMeV [4]. Even though uncertain due to the reduced counting statistics, the data at 1800 AMeV seem to indicate that this invariance possibly extends to much higher bombarding energies.

The evolution of the slope temperatures with angle is shown in Fig. 4. A forward peaking is observed for the high-temperature component of protons ($T2$) and for the ^{7}Li ions. But, while the lithium spectra are only weakly dependent on

the beam energy, signal of a source equilibration, the high-temperature component of the protons ($T2$) is much more sensitive to the beam energy, in particular at forward angles. This is consistent with its origin in the initial cascading stages of the reaction. Results of a comparison with values from the Gudima-Toneev intra-nuclear cascade model [9] are also shown in Fig. 4. The calculated proton yields were sorted into spectra according to the ring structure of the INDRA geometry and fitted with one-source maxwellians. Between 90° and 180°, the experimental and theoretical slope temperatures are in good agreement, confirming that the primary nucleon yields extend into the spectator rapidity regime. However, the model fails to describe quantitatively the rise of the slope temperatures at polar angles smaller than 90°. Whether this discrepancy is due to the particular model used or a more general feature of the approximations made in the intra-nuclear cascade is not yet clear at present. For lithium and fragments in general, it will have to be shown whether the observed angular dependence of the fragment yields and spectra slopes is consistent with emission from a single equilibrated source.

5 Pions

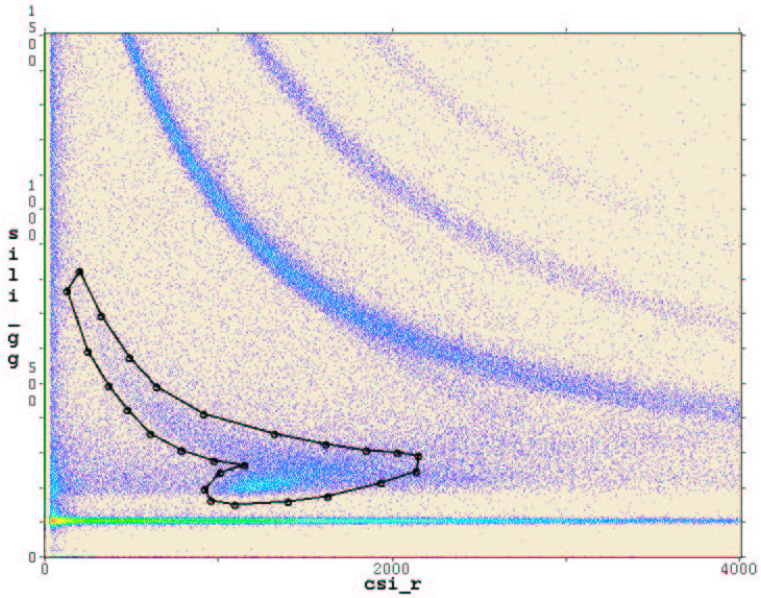

Figure 5: $\Delta E - E$ matrix (in channels) obtained with the Si(Li)-CsI(Tl) detector pair of the calibration telescope of ring 15 ($\langle\theta_{lab}\rangle = 133°$) for $^{12}C+^{197}Au$ reaction at 1000 AMeV. The line gate surrounds the pion branch containing a weak line of stopped $\pi^+(E \leq 68$ MeV) and a rather high peak of more energetic charged pions punching through the detector. The three lines above represent protons, deuterons, and tritons.

For incident beam energies equal to and above 300 AMeV, pions are visible in the Si-Si-CsI(Tl) telescope spectra (Fig. 5), especially at backward angles where the yield of punch-through protons is low.

The weak branch of stopped pions mostly contains π^+ since the capture of π^- leads to considerable additional energy deposits in the CsI(Tl) detector. The pronounced punch-through peak contains both types of charged pions which are also responsible for the background at low ΔE, generated by various reaction processes in the detector.

The pion production, coming from delta resonance creation, is related to an important heating mechanism of the spectator source. As the pion emission is proportional to the number of participants and to the incident energy [10], it might be interesting to search for a potential correlation of the pion and fragment production.

6 Outlook

With the calibration part of the data analysis mostly completed, the physics analysis of the INDRA@GSI experiments has started. First results, so far derived from inclusive particle and fragment yields, demonstrate the usefulness of this detector for fragmentation studies up to the relativistic energy regime.

The preliminary data for light particles and fragments from the ^{12}C+^{197}Au reaction show a gross behavior in agreement with previous ALADIN and EOS results. From the continuing analysis exclusive data are to be expected, complementing the existing data on this asymmetric collision system obtained in inverse kinematics.

References

[1] J. Pouthas et al., Nucl. Inst. and Meth. A 357 (1995) 418

[2] see also: F. Lavaud et al., contribution to this Winter Meeting

[3] see also: J. Łukasik et al., contribution to this Winter Meeting

[4] A. Schüttauf et al., Nucl. Phys. A 607 (1996) 457

[5] C. Gross, PhD thesis, Universität Frankfurt (1998)

[6] J.A. Hauger et al., Phys. Rev. C 57 (1998) 764

[7] S.P. Avdeyev et al., Eur. Phys. J. A 3 (1998) 75

[8] K. Kwiatkowski et al., Phys. Lett. B 423 (1998) 21

[9] V.D. Toneev and K.K. Gudima, Nucl. Phys. A 400 (1983) 173c

[10] J.W. Harris et al., Phys. Rev. Lett. 58 (1987) 463